JOM, Vol. 74, No. 5, 2022
https://doi.org/10.1007/s11837-022-05255-7
© 2022 The Minerals, Metals & Materials Society

TECHNICAL ARTICLE

The Variation of the Electrical Resistance and Microstructure of SnBi based Solder Joints with Current Stressing

FARAMARZ HADIAN,[1] JAVIER FLORES,[1] and ERIC COTTS [1,2]

1.—Physics Department and Materials Science Program, Binghamton University, Binghamton, NY 13902, USA. 2.—e-mail: ecotts@binghamton.edu

Measurements of the electrical resistance of new, SnBi microelectronic interconnects during current stressing were shown to provide sensitive indicators of Bi accumulation at the anode. A linear rate of Bi accumulation at the anode of a SnBi-based solder joint was observed to agree well with a standard electromigration diffusion model. Furthermore, the corresponding increase in the electrical resistance of the solder joint agreed well with a simple model based upon Bi thickness, and with literature values of the electrical resistivity of Bi and eutectic SnBi. The same models provided a specific version of Black's equation for failure (based upon a criterion of a set increase in electrical resistance of the solder joint, e.g., 20%). Good agreement between this equation and the experimental data was found over a range extending from operating temperatures to higher, test temperatures.

INTRODUCTION

The introduction of near-eutectic Sn-Bi for interconnecting microelectronic components has spurred considerable study of the materials science of these Pb-free solders. SnBi solder joints are subjected to current densities exceeding 2000 A/cm^2 and to operating temperatures up to 100 °C.[1,2] Such current stressing of a near-eutectic Sn-Bi solder joint can result in dramatic changes in microstructure, most notably the segregation of Bi to the anode with corresponding changes in the mechanical properties of the solder joint.[3–7] In addition to the formation of a continuous layer of Bi at a linear rate at the anode, intermetallic compounds form at the metallization interfaces, and Bi precipitates coarsen. Furthermore, individual Sn grains have been observed to rotate so that their *A* or *B* axis is aligned with the electrical current direction.[8]

Segregation of Bi at the anode is also correlated with a large increase in the electrical resistance of the solder joint.[9–13] In fact, failure criteria during current stressing focus on specific increases in the electrical resistance of the solder joint, e.g., a 20% increase in the electrical resistance of a SnBi solder joint.[14–17] Thus, characterization of the kinetics of the increase in the electrical resistance of a SnBi solder joint during current stressing should provide a pathway to a quantitative expression for the mean time to failure.

(Received October 11, 2021; accepted March 2, 2022; published online March 31, 2022)

Change In Electrical Resistance as Bi Accumulates at the Anode

The electrical resistivity of Bi is an order of magnitude higher than Sn-Bi based solder, so the formation of a continuous layer of Bi in series with the rest of the solder joint significantly increases the electrical resistance of the solder joint. Relatively simple expressions for the relationship between the change in the electrical resistance and the thickness of the growing Bi layer may be identified. The electrical resistivity of Bi is ten times larger than that of Sn, and four times larger than that of near-eutectic SnBi. An estimate of the change in the electrical resistance, $\Delta R(t)$, in terms of the thickness of the accumulating Bi layer, $y(t)$, is given by:

$$\Delta R(t) = \frac{y(t)}{A}(\rho_{\mathrm{Bi}} - \rho_{\mathrm{SnBi}}) = \frac{y(t)}{A}(100\,\mu\Omega\mathrm{cm}) \quad (1)$$

where A is the cross-sectional area of the solder joint (measured at the anode metallization in this simple model), and ρ_{Bi} and ρ_{SnBi} are the electrical resistivities of Bi and SnBi, respectively, and we assume

cylindrical symmetry. Observed values of $\Delta R(t)$ would be expected to exceed those predicted by Eq. 1, as the value of ρ_{Bi} corresponds to a pristine sample, and Bi accumulating at the anode would be expected to contain a large number of defects. In a treatment that considers only the resistance of the SnBi solder and the Bi segregated at the anode, one may use Eq. 2 to find an expression for $\Delta R/R_o$:

$$\frac{\Delta R(t)}{R_o} = \frac{y(t)}{h}\left(\frac{\rho_{Bi}}{\rho_{SnBi}} - 1\right) = \frac{y(t)}{h}3 \quad (2)$$

where h is the height of the column of SnBi solder, and R_o is the initial resistance of the SnBi solder column (we assume that $R_o = h\rho_{SnBi}/A$). Certain values (e.g., 20%) of $\Delta R/R_o$ are often utilized as a failure criterion during current stressing. The use of such a failure criterion introduces a dependence of the failure time (the time to a particular value of y, i.e., the time to a particular value of $\frac{\Delta R(t)}{R_o}$) on the geometry of the solder joint (i.e., in Eq. 2, $\frac{\Delta R(t)}{R_o}$ depends up on h).

The formation of intermetallic compounds (IMCs) at solder/metallization interfaces would be expected to increase the resistance of SnBi solder joints, albeit at a much slower rate than the formation of a continuous layer of Bi at the anode. The IMCs expected to be formed at Ni or Cu interfaces include Ni_3Sn_4 and Cu_3Sn/Cu_6Sn_5, respectively. The electrical resistivities of these intermetallic compounds are actually less than that of SnBi, but IMC growth is predominantly in the metallization. Thus, one would expect a net increase in the electrical resistance of the solder joint. An estimate of the change in the electrical resistance, $\Delta R_{IMC}(t)$, in terms of the thickness Cu consumed, $z(t)$, is given by:

$$\Delta R_{IMC}(t) = \frac{z(t)}{A}\left(\rho_{Cu_6Sn_5} - \rho_{Cu}\right) = \frac{z(t)}{A}16\,\mu\Omega\text{cm} \quad (3)$$

where A is the cross-sectional area of the solder joint (measured at the anode metallization in this simple model), $\rho_{Cu_6Sn_5}$ and ρ_{Cu} are the electrical resistivity of Cu_6Sn_5 and Cu, respectively, and we assume cylindrical symmetry. Since past research has shown that at any given time, t, $z(t)$ is significantly smaller (approximately four times) than $y(t)$,[18] and the change of electrical resistivity (see Eqs. 1 and 3) is a factor of six smaller, this contribution to the change in the electrical resistance of the solder joint would be expected to be approximately 20 times less than that corresponding to Bi accumulation.

Equations 1, 2 and 3 indicate that the ability to predict $y(t)$ for a particular solder joint would provide the means to predict current-stressing failure times. For instance, the failure criterion $\frac{\Delta R(t)}{R_0} = 0.2$, together with Eq. 2, means that failure would correspond to a particular value of y. Previous researchers have formulated a quantitative expression for the flux of Bi atoms in Sn, J_{Bi}, during current stressing (Eq. 4), and utilized J_{Bi} to formulate an expression for $y(t)$. Using the failure criterion for current stressing and Eqs. 2 and 4, one may build a quantitative expression for the mean time to failure (MTF). We first examine the expression for J_{Bi} during current stressing of near-eutectic SnBi based solder joints.

Bi Flux in Sn as a Function of *j*, *T*, and Composition

Previous investigators have observed constant Bi accumulation rates upon current stressing Sn-Bi-based solder joints (current densities up to 7 kA/cm^2, with ambient temperature ranging from 35 to 70 °C).[3,7,19–23] The solubility limit of Sn in Bi is very low at all temperatures below the melting point of Bi, and the diffusion constant for Sn in Bi is relatively low,[24] so we ignore the motion of Sn in Bi, and focus on the diffusion of Bi in Sn. In the analyses of their experimental data, these previous investigators assumed that J_{EM} dominated J_{Bi}:

$$J_{Bi} = J_{EM} = \frac{Ce\rho_{Sn(Bi)}}{k} DZ^{*}\frac{j}{T} \quad (4)$$

where C is the concentration of Bi atoms in Sn, D is the diffusion coefficient of Bi atoms in Sn, k is the Boltzmann constant, T the absolute temperature, Z^* the effective charge number, e the electronic charge, j the current density and $\rho_{Sn(Bi)}$ the electrical resistivity of the Sn with an equilibrium concentration of Bi.

Examination of possible contributions to J_{Bi} indicates that, under the standard field and testing conditions (50 °C ≤ T ≤ 125 °C, j ≤ 7 kA/cm^2) that SnBi solder joints generally encounter during current stressing, J_{EM} will dominate J_{Bi}, although exceeding these ranges, such as greatly increasing j, can result in significant contributions to J_{Bi} from other terms (Eq. 5). Previously, expressions for J_{Bi} have been developed[25] which illustrate a number of different driving forces for the diffusion of Bi in Sn:

$$J_{Bi} = J_{EM} + J_D + J_{SM} + J_{TM} = \frac{CD}{kT}Z^{*}e\rho j - D\frac{dC}{dx} - \frac{CD}{kT}\Omega^{*}\frac{d\sigma}{dx} - \frac{CD}{kT^2}Q^{*}\frac{dT}{dx} \quad (5)$$

assuming rotational symmetry about the x axis. Here, J_{EM} is driven by an electric field, ρj, J_D by a concentration gradient, $\frac{dC}{dx}$, J_{SM} by a stress gradient, $\frac{d\sigma}{dx}$ and J_{TM} stems from a temperature gradient, $\frac{dT}{dx}$, while Q^* is a constant (called the heat of transport), and Ω^* is a constant, often taken to be the atomic volume. D is assumed to be of the form:

$$D = D_0\exp\left(\frac{E_D}{kT}\right) \quad (6)$$

where E_D is an activation energy for Bi diffusion in Sn, and D_0 is a prefactor. An examination of each of the terms in Eq. 5 provides some insight into the possible influence of the corresponding forces on the diffusion of Bi in SnBi solder joints.

Stress Gradient

In the absence of physical constraints, the stress gradient in Eq. 5, and thus the J_{SM} term, would be expected to be essentially zero throughout the experiment.[26–28] The expectation was that any mechanical stresses created by the diffusion of Bi atoms to the anode of the Sn-Bi samples would be relieved through strain, no stress gradients would persist in the sample, and J_{SM} would remain close to zero. One may note that previous work has shown that in Sn-Bi samples which are physically constrained, for instance by underfilling, retardation of the Bi diffusion does result;[10,12,20,29] plots of Bi drift velocity versus j showing negative y intercepts of magnitude greater than 3×10^{-10} cm/s were observed. This meant that at current densities of up to approximately 4 kA/cm^2, no Bi flux toward the anode was observed. One may examine the dependence of the Bi drift velocity versus j to provide insight into the magnitude of J_{SM}.

Temperature Gradient

We expect that the temperature gradient will be finite near the anode throughout the accumulation of Bi at the anode, but relatively small, such that J_{TM} will be much smaller than J_{EM}. A constant current through a SnBi solder joint will create a temperature gradient, $\frac{\partial T}{\partial z}$, along the length of the solder joint, with a magnitude proportional to j^2. Assuming one-dimensional heat flow from the mid-point of the solder joint along the z direction of the solder joints (i.e. the height direction) toward the anode, the maximum thermal gradient will be given by:

$$\frac{\partial T}{\partial z} = \frac{\rho h j^2}{2\kappa} = 8 \times 10^{-7} j^2 \frac{K}{\mathrm{cm}} \quad (7)$$

where κ corresponds to the thermal conductivity of the SnBi solder, and the units of j are amps/cm^2. We note that, given the symmetry of the test vehicle in the z direction, a similar temperature gradient will exist near the cathode, but with an opposite sign (i.e., in this simple picture, the temperature will be lowest near the cathode and the anode). Thus, for a current density of 4×10^3 amps/cm^2, at temperatures near 100 °C, the maximum temperature gradient would be 13 K/cm. In a previous study, a thermal gradient greater than 1300 K/cm was imposed upon SnBi-based solder joints at a temperature of 120 °C for 300 h, resulting in an accumulation of less than approximately 5μm of Bi. The indication is that J_{TM} for a thermal gradient of 13 K/cm would be relatively small in the present experiments. In fact, a value of Q* of 177 J/mol (cf. Eq. 5) has been reported in the Shen study.[30] Assuming a value for Z^* of 10 for Bi in Sn, the ratio of J_{TM}/J_{EM} for Bi in Sn would be 10^{-4} for $j = 4 \times 10^3$ amps/cm^2, also indicating that J_{EM} is significantly more than J_{TM} for the present study. Such a calculation can be tested through examination of plots of drift velocity versus j.

Concentration Gradient

In the absence of a Bi concentration gradient in the Sn near the anode in the SnBi solder joints, the J_D term (Eq. 5) would be zero. The Sn-Bi samples in the present study initially contained relatively high concentrations of Bi (close to 57 wt%), which result in the presence of Bi precipitates that provide sources of Bi to maintain the average Bi concentration near the anode at the solubility limit. Upon reaching a given temperature, the Bi concentration in the Sn would readily attain the solubility limit everywhere, such that no Bi concentration gradient would exist $\left(\frac{dC}{dx} = 0\right)$, and the $D\frac{dC}{dx}$ term would not contribute to J_{Bi}. If J_{EM} dominates J_{Bi}, there would be a constant flux everywhere except the boundaries (anode and cathode) of the solder joint, and this concentration profile, with $\frac{dC}{dx} = 0$, would be maintained. Such an assumption can be tested through examination of Bi concentrations as a function of position after current stressing to provide insight in to the magnitude of J_D.

CALCULATED RATE OF BI ACCUMULATION AT THE ANODE, *Y(T)*

Previous investigators have assumed that J_{EM} dominates J_{Bi}, and have used Eq. 4 to develop expressions for the thickness, $y(t)$, of a Bi-layer accumulating at the anode versus time.[7,19] In our development of an expression of an expression of MTF as a function of j and T, we also assume that J_{EM} dominates J_{Bi}, and then compare the resulting expression to experimental data. The first step is to relate J_{EM} to $y(t)$. This includes a calculation of the number of Bi atoms already present in the Sn near the anode:[7,19]

$$\begin{aligned} y(t) &= J_{EM} V_m \left(1 + \frac{N_{Bi}}{N_{Sn}}\right) t \\ &= \frac{e\rho V_m}{kN_A}\left(1 + 0.57\frac{X_{Bi}}{X_{Sn}}\right) \mathrm{CDZ}^* \frac{j}{T} t = bt \end{aligned} \quad (8)$$

using the molar volume of Bi, V_m, the number of Bi atoms, N_{Bi}, and the number of Sn atoms, N_{Sn} in the solder (see Eq. 3). Assuming the temperature, the current density and the solder composition are each constant, the quantity b in Eq. 8 is a constant. Here, the weight percentages of Bi and Sn in the solder (X_{Bi} and X_{Sn}, respectively) were used to provide a form of the expression more easily utilized with the standard nomenclature for commercial solders:

$$\frac{N_{\mathrm{Bi}}}{N_{\mathrm{Sn}}} = 0.57\frac{X_{\mathrm{Bi}}}{X_{\mathrm{Sn}}} \tag{9}$$

using the molar masses of Bi and Sn. Values for D have been previously measured as a function of temperature.[31]

Calculated Expression for the Mean Time to Failure During Current Stressing

Given that standard failure criteria for SnBi solder joints depend upon attaining particular values of $\frac{\Delta R(t)}{R_o}$ (e.g., $\frac{\Delta R(t)}{R_o} = 0.2$), that Eq. 2 directly relates $\frac{\Delta R(t)}{R_0}$ to $y(t)$, and that Eq. 8 provides a quantitative expression for $y(t)$, one may derive an analytical expression for the mean time to failure for SnBi-based solder joints. One finds that, substituting Eq. 8 in Eq. 2 and defining MTF as the time when $\frac{\Delta R(t)}{R_o} = 0.2$, then MTF is given by:

$$\mathrm{MTF} = \frac{B}{j}\exp\left(\frac{E_D}{\mathrm{kT}}\right), \tag{10}$$

where

$$B = \frac{0.2kN_A hT}{\left(\frac{\rho_{\mathrm{Bi}}}{\rho_{\mathrm{SnBi}}} - 1\right)e\rho_{\mathrm{Sn(Bi)}}V_m CD_o Z^*\left(1 + 0.57\frac{X_{\mathrm{Bi}}}{X_{\mathrm{Sn}}}\right)} \tag{11}$$

Black's Equation

The expression for MTF as a function of j and T (Eq. 10) displays a number of similarities to Black's equation:

$$\mathrm{MTF} = \frac{A'}{j^n}\exp\left(\frac{E_a}{\mathrm{kT}}\right), \tag{12}$$

where A' and E_a are constants (E_a is identified as an activation energy,[32] although not tied to solely to the diffusion process). It is clear from examination of Eq. 10 that it would be expected that $n = 1$. That is to say, because $B(T)$ (Eq. 11) varies relatively slowly over the temperature range of interest ($80 < T < 130$ °C), one would also expect that data obeying Eq. 10 could be fit via Black's equation, but that $E_a \neq E_D$, and $A' \neq B(T)$. In other words, the temperature dependence of $B(T)$ would be captured in exponential function through use of $E_a \neq E_D$. One may examine the dependence of MTF on j and T and consider the efficacy of both Eqs. 10 and 12.

THE PRESENT STUDY

For near-eutectic SnBi based solder joints, we sought to experimentally characterize MTF as a function of j and T, for a failure criterion of a 20% increase in the electrical resistance of the solder joint, and to compare our results to the associated physical processes reflected in Eqs. 1–12. We sought to determine how the accumulation of Bi at the anode corresponds to the change of the electrical resistance of the solder joint, and to determine values of MTF as a function of j and T. We sought to compare this dependence of MTF on j and T to Eqs. 10, 11 and 12, and therefore, to compare the results of a simple model based upon electromigration theory (Eqs. 10 and 11) to the more generic Black's equation (Eq. 12).

EXPERIMENTAL PROCEDURE

In this work, four terminal measurements of the electrical resistance versus time of Sn57BiSbNi solder joints were performed while they were stressed with a constant direct current, at a constant temperature (Sb and Ni were present in concentrations significantly less than one wt%). Sn57BiSbNi solder paste was used to assemble two different geometries of cylindrical solder joints, using a conventional surface mount technology process. The first samples consisted of a daisy chain row of eight, 200 μm-diameter, non-solder mask defined solder joints, each with a laminate board and a small chip (S1, sample one). The second samples were individual, 230 μm-diameter, solder mask defined solder joints, each with a custom-made laminate chip on a laminate board (S2, sample two). The S2 sample geometry provided four terminal measurements of the electrical resistance of individual solder joints. For both samples, the metallization on the component side was Ni, with a Cu metallization on the board. Thus, Ni/Sn57Bi0.5SB0.01Ni/Cu solder joints were assembled. The solder joints themselves were utilized as thermometers, using the TCR method (JESD33B).[33] A Pt RTD thermometer was utilized in close contact to a solder joint under stress to confirm the temperature calibrations. Measurements of the temperature of the SnBi based solder joints were recorded as a function of current density and ambient temperature.

RESULTS

Resistance Versus Time During Current Stressing

Current stressing SnBi-based low-temperature solder joints at temperatures between 85 and 125 °C with current densities between 2 and 7 kamps/cm^2 resulted in large, monotonic increases in their electrical resistance (e.g., Fig. 1). Four terminal electrical resistance measurements of thirty different individual S2 solder joints during current stressing Fig. 1b revealed large increases over the first 700 h of current stressing. It was evident that there was significant scatter in both the initial electrical resistance, R_o, of each near-

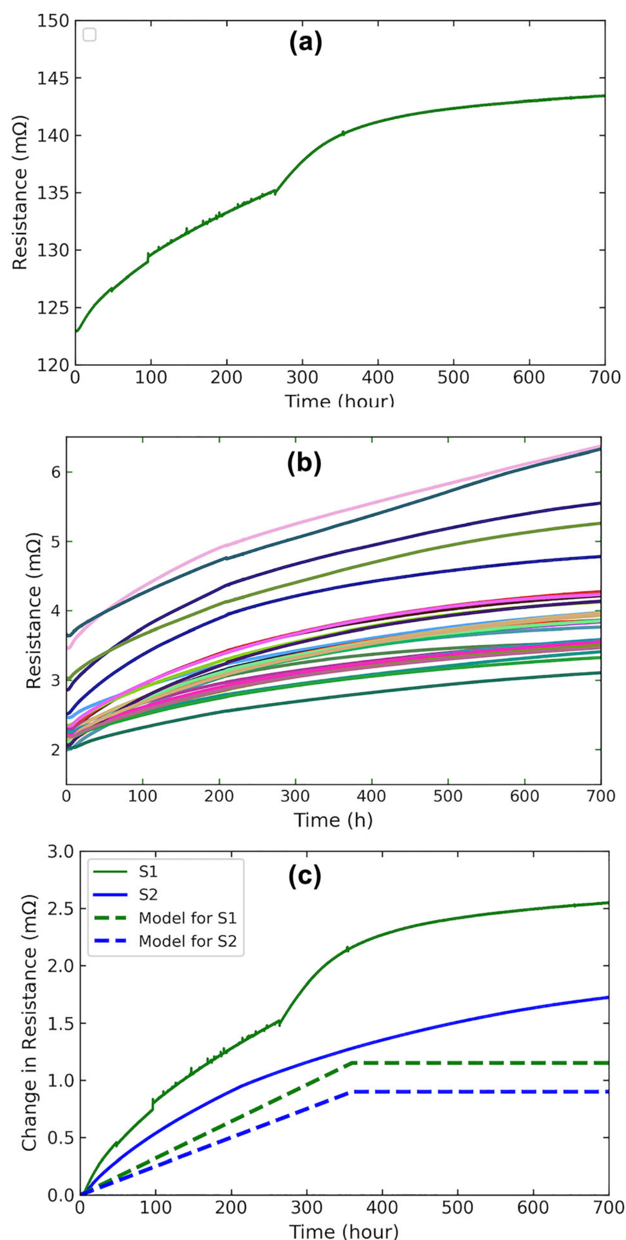

Fig. 1. Plots of the electrical resistance versus time for: (**a**) eight sample S1 (Sn57Bi0.5SB0.01Ni) solder joints connected in series. The current density in these samples was 4 kA/cm^2 and the temperature 123 °C. (**b**) Four terminal measurements of the electrical resistance of individual sample S2 solder joints (Sn57Bi0.5SB0.01Ni) under current stressing of 4 kA/cm^2 at a temperature of 125 °C. (**c**) Solid lines plots of the change in average electrical resistance versus time. Green line (upper solid curve)—the data from (**a**) with the electrical resistance at time zero subtracted, divided by eight, the number of solder joints in series. Blue line (lower solid curve), average of plots garnered from thirty different samples (see plots in (**b**)). Dashed lines are predictions based upon measurements of the thickness of Bi accumulating at the anode (see text) (Color figure online).

eutectic SnBi solder joint, and in the electrical resistance versus time (Fig. 1b). For these data, the electrical resistance at time zero was subtracted, the differences were averaged, and the results were plotted in Fig. 1c (blue, lower solid curve). Examining this plot, an average increase of approximately 4 $\mu\Omega$ per hour was observed in the electrical resistance of S2 solder joints for the first 350 h of current stressing at a temperature of 125 °C and a current density of 4 kA/cm^2 (Fig. 1c, solid blue line). The rate of increase decreased as a function of time. It was approximately 6 $\mu\Omega$ per hour for the first 100 h, while at a time of 350 h the rate of increase had decreased by a factor of two. Between 400 and 700 h the average rate of increase was approximately 1.4 micro-ohm per hour. The average resistance changes of eight S1 solder joints in series (Fig. 1a) were similar, an average increase of 7 $\mu\Omega$ per hour was observed for the first 400 h. The changes in the electrical resistance during current stressing of these solder joints in series were provided by subtracting the initial resistance, and then dividing the data of Fig. 1a for the eight S1 samples in series by eight (Fig. 1c, green, upper solid curve). After 400 h, the electrical resistance of this chain of solder joints continued to increase, but at a reduced rate (Fig. 1).

Accumulation of Bi at the Anode During Current Stressing

The large increases in the electrical resistance of the SnBi-based solder joints during current stressing were correlated with the accumulation of a continuous Bi layer at the anode of the solder joint. For instance, selected S1 solder joints were removed after 100 h of current stressing at a temperature of 123 °C and a current density of 4 kA/cm^2, cross-sectioned and examined with scanning electron microscopy (SEM); Fig. 2. After reflow a very thin layer (less than 0.5 μm) of $(Cu,Ni)_6Sn_5$ intermetallic formed at the solder/Ni interface in the component side. In contrast, around 1.5 μm Cu_6Sn_5 intermetallic formed at the solder/Cu interface in the board side. The solder in the as-reflowed SnBi solder joints consisted of β-Sn, Bi-rich phases with small amount of Cu_6Sn_5 IMCs (Fig. 2a and b). During current stressing, all the IMC's coarsened at the interfaces and within the solder (Fig. 2f). Furthermore, as can be seen in Fig. 2b and e, a substantial layer of Bi (approximately 10 μm in thickness) had accumulated at the anode side of these solder joints. Observations of the Bi layer thicknesses, at different durations of current stressing different Sn57BiSbNi solder joints of both geometries under similar conditions, revealed an essentially linear increase with time for the first 10 days of current stressing, as reflected in the plots of thickness versus time, $y(t)$, in Fig. 3, and a fit to those data (solid line, Fig. 3). The dashed horizontal line in Fig. 3 reflects an estimate of the maximum amount of Bi that can accumulate at the anode, based upon a simple calculation using the known compositions of the solders.

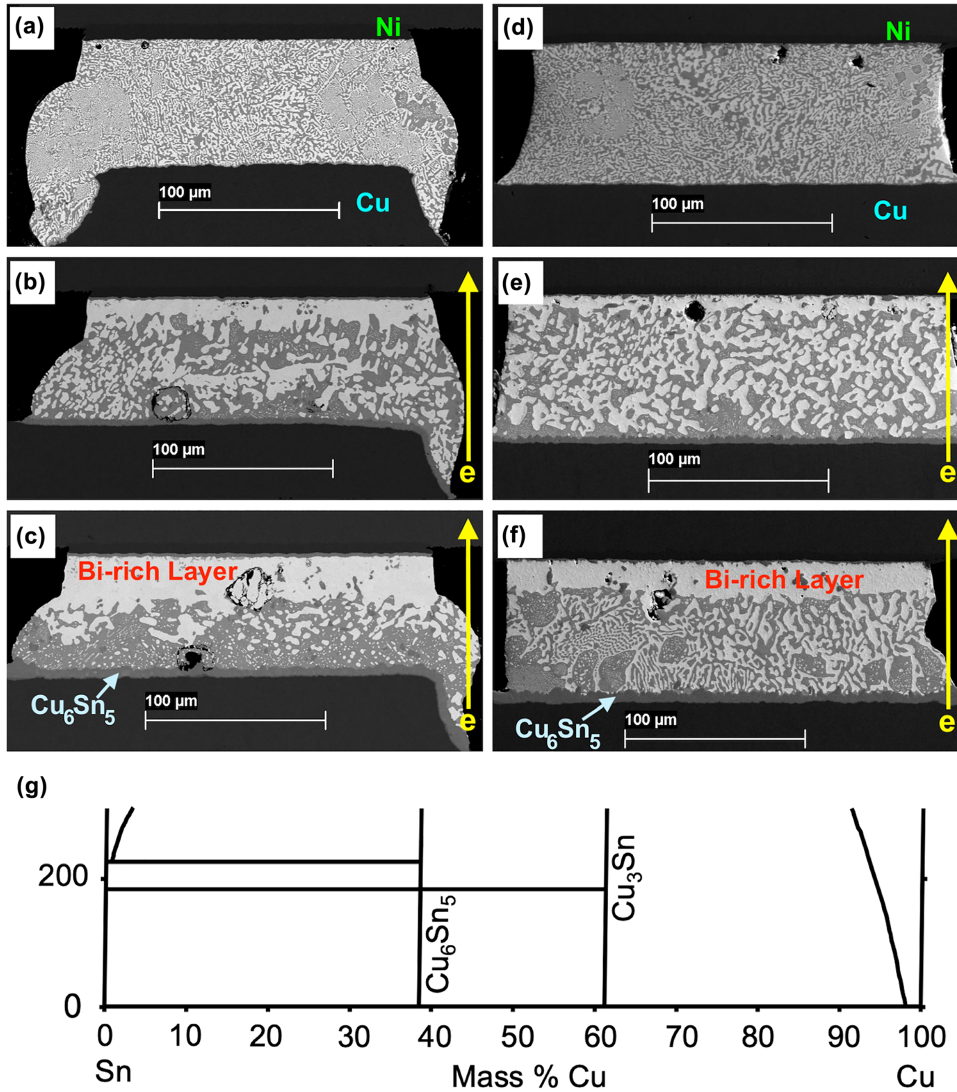

Fig. 2. Microstructure of Ni/ Sn57Bi0.5SB0.01Ni/Cu solder joints in S1after **a** reflow, **b** 100 h and **c** 260 h under current stress of 4 kA/cm2 at 123 °C and in S2 after **d** reflow, **e** 100 h and **f** 200 h under current stress of 4 kA/cm2 at 125 °C **g** Sketch of the Cu-Sn binary phase diagram, with temperatures from 0 to 300 °C and Cu concentration in units of mass percentage.[34–36]

ANALYSIS

Correlation Between Bi Accumulation at the Anode and Change in Electrical Resistance

The increase in electrical resistance observed during the first 400 h of current stressing of a large variety of near-eutectic SnBi-based solder joints (Fig. 1) was correlated with the segregation of Bi to the anode (Figs. 2 and 3). As the thickness of the Bi layer accumulated at the anode increased to 40 μm over a period of approximately 400 h (Fig. 3), the average electrical resistance increased by approximately 1.3 mΩ, or at a rate of approximately 0.33 Ω/cm. This observation can be compared to the prediction of Eq. 1: $\Delta R(t) = (0.23\ \Omega/\text{cm})\ y(t)$. Predictions of the change in electrical resistance of the solder joints during current stressing based upon Eq. 1 and the observed thickness changes in the Bi are included in Fig. 1c (no fitting was performed). The observed slope is higher than expected on the basis of Eq. 1. Perhaps most interesting, when Bi ceased accumulating at the anode (at a time of approximately 400 h), the electrical resistance of the SnBi-ased solder joint continued to increase at a rate of approximately 1.4 micro-ohm per hour. It was observed that the Cu_6Sn_5 phase (Fig. 2g) grew at the SnBi solder/Cu interface, and at the SnBi solder/Ni interface, in the form of $(Cu, Ni)_6Sn_5$. In fact, similar growth has been previously observed in Cu/(Sn-based solder)/Ni solder joints.[37–39] The increase in the electrical resistance of the SnBi-based solder joint at times greater than 400 h was correlated with this increasing thickness of Cu-Sn intermetallic compounds, although at a rate more than five times higher than predicted by Eq. 3. The fact that the values of the electrical resistance of the SnBi based solder joint are larger than expected by

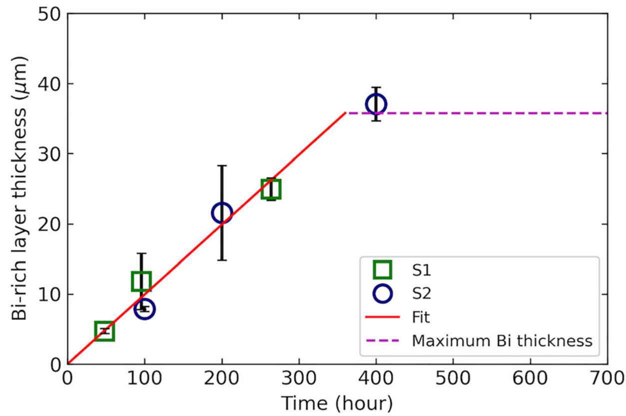

Fig. 3. Plot of accumulated Bi thickness as a function of time for Ni/ Sn57Bi0.5SB0.01Ni /Cu solder joints with two different geometries; red squares S1, and green circles S2. A calculation of the maximum amount of Bi that could accumulate at the anode is included as a dashed line. A fit to all of data for accumulated Bi thicknesses less than the calculated maximum thickness is shown by solid line (Color figure online).

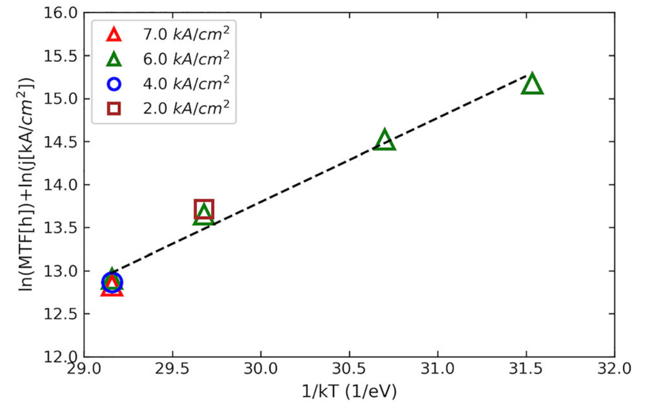

Fig. 4. The natural logarithm of the mean time to failure (MTF) times the current density versus the inverse of Boltzmann's constant times the temperature, where failure during current stressing was determined by a 20% increase in the electrical resistance of the solder joint. Data were compiled at a current density between 2 and 7 kA/cm^2, as indicated in the legend.

Eqs. 1–3 may simply reflect the fact that electrical resistances are highly sensitive to the presence of defects, both structural and chemical. In any event, the four terminal measurements of the change in the resistance of these SnBi solder joints provide a sensitive means to estimate the thickness of the Bi layers forming at the anode during current stressing (Eq. 1).

Mean Time to Failure Versus j and T

The results of the present investigation (Eqs. 1, and 12) provide the means to formulate a quantitative expression for the (MTF) using an increased resistance criterion for these SnBi-based solder joints, in terms of current density, temperature, and solder joint height, including a common form of Black's equation (Eq. 13). Current stressing of a near-eutectic Sn-Bi solder joint (Fig. 1) caused the electrical resistance of a SnBi-low temperature solder joint to increase by much more than 20% (a standard criterion for failure of a joint, particularly for solder joints which have not been underfilled). The four terminal measurements of the change in the resistance of these SnBi solder joints provided a highly sensitive means to measure this change in electrical resistance during current stressing (Fig. 1). Excursions of the change in electrical resistance to values greater than 20% of the initial electrical resistance of the SnBi solder joint were clear (Fig. 1). Measurements of MTF were performed at different temperatures, ranging from 95 to 125 °C, and current densities, ranging from 2 to 7 kA/cm^2.

These data are presented in Fig. 4, a plot of the natural logarithm of the current density plus the natural logarithm of the MTF, versus the inverse temperature (Eq. 12, Black's equation). The data for different values of j, but the same value of T, essentially coincided with each other in this plot, consistent with an inverse relation between MTF and j, as indicated in Eqs. 10 and 12 (with a value of 1 adopted for the quantity n). A linear fit to all of the data of Fig. 4 was performed, and is provided in the figure as a dashed line, the slope of which indicated a value of E_a = 0.98 eV. That is to say, these data could be well characterized by the form of Black's equation presented in Eq. 12 (where, for Black's equation, A' is assumed to be independent of temperature), with

$$\mathrm{MTF} = \frac{1.9 \times 10^{-7}}{j} \exp\left(\frac{0.98}{kT}\right) \text{ hours} \tag{13}$$

The same MTF (j, T) data were fit using Eqs. 10 and 11, and the value of E_D was found to be 0.74 eV, consistent with previous measurements of the diffusion constant of Bi in Sn.[31] A similar quality of linear fit was found using either Eqs. 10 and 11, or Eq. 12, in characterizing the temperature and current density dependence of the mean time to failure. Furthermore, extrapolations of MTF models were made to temperatures below 95 °C. For temperatures between 65 and 95 °C, similar values (i.e., within 1%) of MTF were found using either approach. As temperatures decreased below 65 °C, values of MTF predicted by each approach began to diverge; at a temperature of 50 °C the MTF predicted by Eqs. 10 and 11 was 10% less than that predicted by Black's equation (Eq. 12). Thus, over a limited temperature range of extrapolation, the simpler approach as found in Black's equation (Eqs. 12 and 13) was found to provide similar results to the more complex formulation of Eqs. 10 and 11. The observation that the model of Eqs. 10 and 11 fit the observed data with a value of E_D similar to that found in studies of diffusion driven only by a concentration gradient is consistent with the conclusion that J_{EM} dominates J_{Bi}.

Contributions to J_{Bi}

The observations of changes in the electrical resistance and microstructure of near-eutectic SnBi solder joints current-stressed at temperatures between 95 and 125 °C and at current densities up to 7 kA/cm^2, were consistent with the domination of J_{Bi} by J_{EM}. In Fig. 2 the temperature gradient was in the same direction as electron current at the anode, but in an opposite direction to the electron current at the cathode. Bi readily accumulated at the anode, while no Bi accumulated at the cathode; in fact, some depletion of Bi was observed at the cathode (Fig. 2). Thus, $J_{EM} >> J_{TM}$. The dependence of MTF and of the drift velocity on j support this contention, as well as a contention that $J_{EM} >> J_{SM}$. The value of MTF for a given temperature was observed to be directly proportional to the inverse of the current density (Fig. 4), consistent with Eqs. 10 and 12, for current densities ranging from 2 kA/cm^2 to 7 kA/cm^2. As pointed out above, this is evident in Fig. 4, where for each of the higher two temperatures examined, ln(MTF) + ln(j) was essentially the same for the two or three different values of the current density that were utilized. In Fig. 5, these data are replotted in the form of drift velocity versus current density, where the magnitude of drift velocities for samples current stressed in the present study were estimated from measurements of R versus time at a constant temperature. In Fig. 5, these data are compared to a previous result from the work by Wang et al.,[20] where Sn-Bi-based solder joints were encapsulated in underfill in an effort to constrain expansion and therefore limit Bi diffusion. While the linear fits to the data from the present study coincide with the origin (within experimental error), there is a significant offset in the data for the samples which were physically constrained, in the previous study. The observation that the drift velocities observed in the present study are linearly dependent upon j is consistent with the conclusion that J_{EM} dominates J_{Bi}.

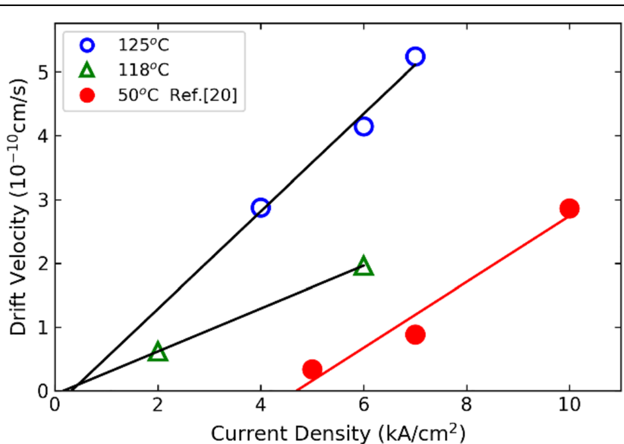

Fig. 5. Plot of an estimate of the drift velocity of Bi atoms in Sn versus current density for SnBi-based solder samples, at constant temperature: open circles, 125 °C; open triangles, 118 °C. Data from a previous investigation by Wang et al.[20] are provided as closed circles. The ambient temperature for the data from Wang et al. was reported to be 50 °C, with the actual temperature of the sample significantly higher due to Joule heating.

The high quality of the linear fit to the data of Fig. 4 lends credence to the applicability of Eqs. 10, 11 and 12 to various field conditions. The observation that J_{EM} dominates J_{Bi} provides credence to the assumption of previous investigators that Eq. 4 is applicable in describing the accumulation of Bi at the anode during the current stressing of SnBi-based solder joints. Given a simple fundamental basis for Eqs. 10, 11 and 12, extrapolations of these equations to lower temperatures should be quite reasonable. Perhaps most importantly, identification of the parameters of Black's equation at higher temperatures has been shown to allow calculation of MTF at lower temperatures thereby enabling the determination of acceleration factors for laboratory current stressing.

CONCLUSIONS

Four terminal measurements of the electrical resistance of SnBi solder joints were shown to be sensitive to Bi accumulation. A direct correlation between the change in the electrical resistance of SnBi-based solder joints and Bi accumulation at the anode during current stressing, was observed. Thus, previously identified expressions for the flux of Bi atoms in Sn during current stressing can be used to develop quantitative expressions for the change in the electrical resistance of SnBi-based solder joints having various compositions and dimensions as a function of time, temperature, and current density. The experimental data of the present study were found to be consistent with models that assume that J_{EM} dominates J_{Bi}.

Because many current-stressing failure criteria depend upon particular changes in the electrical resistance of SnBi-based solder joint, a quantitative expression for MTF as a function of j and T was identified (using the criterion of 20% increase in electrical resistance as a specific example). This expression was Arrhenius in nature, with an activation energy of 0.74 eV, and a proportionality coefficient between MTF and the exponential function that was temperature dependent. This expression was well captured as a form of Black's equation with n = 1 (MTF inversely proportional to j) and an apparent activation energy of 0.98 eV. Thus, an expression for MTF in the form of Black's equation was quantitatively determined for this system. This formalism provides clear MTF acceleration factors for laboratory current stressing of such-low temperature solder joints.

ACKNOWLEDGEMENTS

Partial support from the Semiconductor Research Corporation is gratefully acknowledged. Partial support from the Universal Instruments AREA

Consortium is gratefully acknowledged. The authors are indebted to Michael Meilunas of Universal Instruments Corporation for the design and fabrication of all test coupons used in this study. We gratefully acknowledge James Wilcox of Universal Instruments for important discussions.

CONFLICT OF INTEREST

The authors state that there is no conflict of interest.

REFERENCES

1. S.P. Lim, C. Arvin, D. Locker, R. Pokhrel, W.K. Loh, K. Sweatman, D. Daily, N. Kubota, and M. Tsuriya, *Int. Conf. Electron. Packag. ICEP* 2021, 49 (2021).
2. J. Glazer, *J. Electron. Mater.* 23, 693 (1994).
3. L.T. Chen, and C.M. Chen, *J. Mater. Res.* 21, 962 (2006).
4. Q.L. Yang, and J.K. Shang, *J. Electron. Mater.* 34, 1363 (2005).
5. K.N. Tu, *Springer Ser. Mater. Sci.* 117, 245 (2007).
6. S. Sahasrabudhe, S. Mokler, M. Renavikar, S. Sane, K. Byrd, E. Brigham, O. Jin, P. Goonetilleke, N. Badwe, S. Parupalli, in *2018 IEEE 68th Electronic Components and Technology Conference (ECTC)* (IEEE, 2018), pp. 1455–1464.
7. X. Gu, and Y.C. Chan, *J. Electron. Mater.* 37, 1721 (2008).
8. A.T. Wu, A.M. Gusak, K.N. Tu, and C.R. Kao, *Appl. Phys. Lett.* 86, 1 (2005).
9. X. Zhao, M. Saka, M. Muraoka, M. Yamashita, and H. Hokazono, *J. Electron. Mater.* 43, 4179 (2014).
10. F. Guo, G. Xu, J. Sun, Z. Xia, Y. Lei, Y. Shi, and X. Li, *J. Electron. Mater.* 38, 2756 (2009).
11. J. Sun, G. Xu, F. Guo, Z. Xia, Y. Lei, Y. Shi, X. Li, and X. Wang, *J. Mater. Sci.* 46, 3544 (2011).
12. X. Zhao, M. Muraoka, and M. Saka, *J. Electron. Mater.* 46, 1287 (2017).
13. G. D. Pilin Liu, F. –Y. Ouyang, S. Qu, Z. Fu, in *ASME 2009 InterPACK Conf. Proc. IPACK2009* (2009), pp. 1–7.
14. JEDEC Solid State Technol. Assoc (2011).
15. S.M. Lee, J.W. Yoon, and S.B. Jung, *J. Mater. Sci. Mater. Electron.* 27, 1105 (2016).
16. W.J. Choi, E.C.C. Yeh, and K.N. Tu, *J. Appl. Phys.* 94, 5665 (2003).
17. J. Pan, J. Silk, 44th Int. Symp. Microelectron. 2011, IMAPS 2011 **2**, 694 (2011).
18. M.S. Park, and R. Arroyave, *J. Electron. Mater.* 39, 2574 (2010).
19. C.M. Chen, L.T. Chen, and Y.S. Lin, *J. Electron. Mater.* 36, 168 (2007).
20. F. Wang, L. Liu, D. Li, and M. Wu, *J. Mater. Sci. Mater. Electron.* 29, 21157 (2018).
21. W. Zhou, L. Liu, B. Li, and P. Wu, *Thin Solid Films* 518, 5875 (2010).
22. S. Ismathullakhan, H. Lau, and Y.C. Chan, *Microsyst. Technol.* 19, 1069 (2013).
23. J.H. Kim, Y.C. Lee, S.M. Lee, and S.B. Jung, *Microelectron. Eng.* 120, 77 (2014).
24. P.T. Vianco, and J.A. Rejent, *J. Electron. Mater.* 28, 1127 (1999).
25. J.R. Lloyd, *Microelectron. Eng.* 49, 51 (1999).
26. I.A. Blech, and C. Herring, *Appl. Phys. Lett.* 29, 131 (1976).
27. I.A. Blech, *J. Appl. Phys.* 47, 1203 (1976).
28. I.A. Blech, *Acta Metall.* 46, 3717 (1998).
29. X. Zhao, S. Takaya, and M. Muraoka, *J. Electron. Mater.* 46, 4999 (2017).
30. Y.A. Shen, S. Zhou, J. Li, K.N. Tu, and H. Nishikawa, *Mater. Des.* 166, 107619 (2019).
31. A.M. Delhaise, Z. Chen, and D.D. Perovic, *JOM* 71, 133 (2019).
32. J. R. Black, in *2005 IEEE Int. Reliab. Phys. Symp. 2005. Proceedings. 43rd Annu.* (IEEE, 1967), pp. 1–6.
33. JEDEC, JESD33B, (2012).
34. S. Fürtauer, D. Li, D. Cupid, and H. Flandorfer, *Intermetallics* 34, 142 (2013).
35. D. Li, P. Franke, S. Fürtauer, D. Cupid, and H. Flandorfer, *Intermetallics* 34, 148 (2013).
36. W. Zhao, Y. Yang, E. Zhang, B. Zhang, M. Wen, Y. Tang, and L. Zhang, *Calphad Comput. Coupling Phase Diagr. Thermochem.* 75, 102344 (2021).
37. C.W. Chang, S.C. Yang, C. Te Tu, and C.R. Kao, *J. Electron. Mater.* 36, 1455 (2007).
38. S.W. Chen, S.H. Wu, and S.W. Lee, *J. Electron. Mater.* 32, 1188 (2003).
39. K.N. Reeve, J.R. Holaday, S.M. Choquette, I.E. Anderson, and C.A. Handwerker, *J. Phase Equilibria Diffus.* 37, 369 (2016).

Publisher's Note Springer Nature remains neutral with regard to jurisdictional claims in published maps and institutional affiliations.